Electon Tomography

DOI: 10.1002/anie.201303804

Electron Tomography: Three-Dimensional Imaging of Real Crystal Structures at Atomic Resolution**

*Bingsen Zhang and Dang Sheng Su**

atomic resolution · catalysis · electron tomography · nanostructures · structure determination

Transmission electron microscopy (TEM) acts as the scientist's "electronic eyes" as it not only reveals the morphology, but also provides structural, chemical, and electronic information on nanomaterials at the atomic level. This information provides a dramatic driving force for the development of nanoscience and nanotechnology.[1–9] TEM and high-resolution TEM, however, generate only two-dimensional (2D) projections through a three-dimensional (3D) structure, as shown in Figure 1 a. Information about the real 3D structure—such as the exposure surface, internal structure, surface defects, and 3D shape of a gold nanoparticle (Au NP; see Figure 1 b)—is missing from a 2D TEM image. It is therefore crucial to obtain the 3D structures, and several indirect methods have been applied, such as the combination of two or more TEM images[5,10] and the serial sectioning of the sample by microtomy[11] accompanied by simulations for reconstructing the structures and shapes of NPs and nanorods.

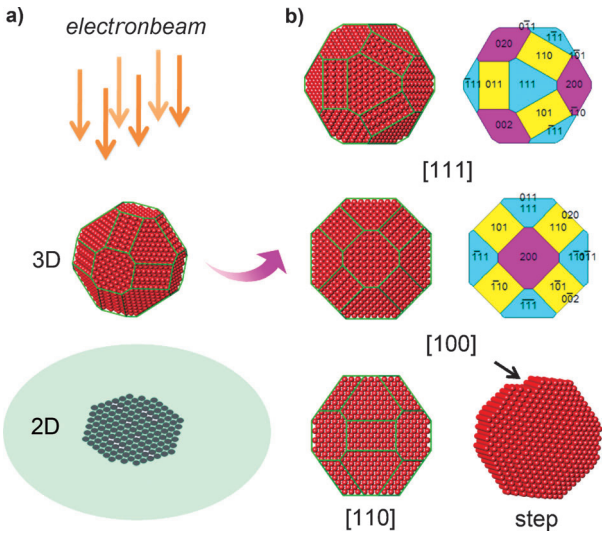

Figure 1. a) Representation of a 2D projection of a 3D gold NP by TEM; b) atomic structure, 3D shape, and surface defect of a gold NP in different orientations.

Besides the aforementioned methods, electron tomography (ET) is a general and effective approach to reconstruct the 3D structures of nano-objects from a tilt series of 2D images.[12–16] Already in 1968, efforts were primarily made to "retrieve" 3D information from 2D TEM projections, but it mainly remained limited to the field of structural biology.[17,18] Its wide popularity as a key aid for the 3D study of morphologies, spatially discriminating chemical compositions, and defect properties of nanostructured materials in other fields (e.g., structural and energy materials) started about a decade ago by the use of scanning transmission electron microscopy (STEM) and TEM. Before 2011 the best resolution in three dimensions was roughly 1 nm,[12] although with spherical-aberration-corrected TEM resolution as low as 0.5 Å[19] is possible for several reasons. First, it is difficult to align the projections of a tomography tilt series to a common axis with atomic-level precision. Second, the tilt range is usually from +75° to −75°, which leads to a "missing wedge" of information that caused an elongation of the reconstruction point-spread function. Last, the damage from the electron beam limits the number of projections that can be acquired from a nano-object.[12,13,20] Therefore, the 3D representation of real crystal structures, including dislocations, stacking faults interfaces, and grain boundaries, remains a challenge .

Recently, significant progress has driven the resolution in three dimensions to the atomic level.[20–23] One approach consists of quantifying the projected intensity of each atomic column by using a best-fit statistical method incorporating the discrete constraint (named discrete tomography (DT));[21] this was the first method showing real 3D tomography with atomic resolution and is very useful for reconstructing the fine 3D structures of small NPs. The DT method assumes prior knowledge of the NP's lattice structure and requires that the atoms fit rigidly on that lattice. Another method combines a center-of-mass (CM) alignment approach and equally sloped tomography (EST) reconstruction method with annular dark-field STEM (ADF-STEM); in this way, the 3D structures of an approximately 10 nm Au NP have been

[*] Dr. B. Zhang, Prof. Dr. D. S. Su
Shenyang National Laboratory for Materials Science
Institute of Metal Research
Chinese Academy of Sciences
72 Wenhua Road, Shenyang 110016 (China)
E-mail: dangsheng@fhi-berlin.mpg.de

[**] We gratefully acknowledge the financial support provided by the IMR SYNL-T.S. Kê Research Fellowship, the National Natural Science Foundation of China (nos. 21203215, 21133010), MOST (2011CBA00504), and the China Postdoctoral Science Foundation (2012M520652).

determined at 2.4 Å resolution.[20] Although the lattice and some individual atoms are visible in the reconstruction, the ET method cannot reveal all of the atoms inside the NP because of dynamic scattering effects, the "missing-wedge" problem, and Poisson noise in the tilt series. Subsequently, in a recent paper published in *Nature*,[24] Chen et al. overcome these obstacles by combining 3D Fourier filtering together with EST tomography in high-angle ADF STEM (HAADF-STEM) mode. The breakthrough lies, for the first time, in the ability to observe nearly all atoms in a roughly 10 nm multiply twinned platinum NP, achieving atomic steps at 3D twin boundaries and imaging the 3D core structure of edge and screw dislocations at atomic resolution. This data give solid support for the existence of the classical 3D block models of crystal defects presented in materials-science lectures, publications, and textbooks.

The EST-based ET in combination with CM alignment and 3D Fourier filtering represents a general method for 3D atomic-resolution imaging of the local structure in NPs.[24] Because of the low signal-to-noise ratio (SNR) in the EST reconstruction, 3D dislocations within the NP cannot be identified at atomic resolution. The proposed 3D Fourier filtering method can identify all the measureable 3D Bragg peaks and the 3D distribution around each peak. With this method nearly all the atoms are visible in a slice of the NP in the *xy* plane.

In Figure 2 the grain boundaries in a 2D experimental projection and in a reconstructed Pt NP composed of 2.6 Å thick internal slices. The NP is multiply twinned with flat twin boundaries (Figure 2a). The atomic steps at the twin boundaries (Figure 2b,c) are hidden in the projection (Figure 2a) and vary in consecutive atomic layers (Figure 2c–e). A stacking fault can be also observed at a twin boundary. Except for the aforementioned structures, the 3D core structure of edge and screw dislocations (see Figure 4 in Ref. [24]) at atomic resolution in the Pt NP can be deduced by applying these approaches, whereas it is not visible in a conventional 2D projection. Considering the location of the screw dislocation inside the Pt NP, the twin boundaries are not flat. The dislocations associated with the atomic steps at the boundaries account for the strain relaxation.[24]

Identifying the real atomic structure is crucial for the development of nanomaterials.[25–27] The new imaging technology is a milestone for the structure analysis of nanomaterials in three dimensions at the atomic level, and may have widespread applications in materials science and nanoscience. For instance, it could become a powerful tool for characterizing surface and internal structures of catalysts in order to establish synthesis–structure–property relationships. With the new development of 3D ET in the future, the electron energy loss spectrum (EELS) may be acquired synchronously. Thus, the 3D electronic structure information of both surface and bulk can also be reconstructed (e.g., bonds, valence state, and composition, as shown in Figure 3). Furthermore, it could be a powerful technique for exploring the "black box" of nanomaterials (e.g., solid catalysts and energy-conversion and energy-storage materials) under working conditions at the atomic and electronic level. This would enable us to design and fabricate nanomaterials with new structures and desired properties at an unprecedented level.

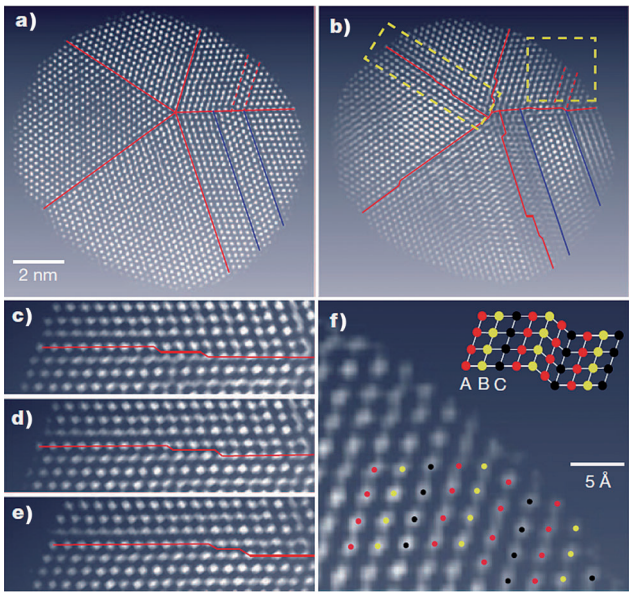

Figure 2. Comparison of grain boundaries in a 2D experimental projection and in a Pt NP reconstructed from several 2.6 Å thick internal slices. a) Experimental projection in the *xy* plane suggesting that this is a decahedral multiply twinned NP and that the twin boundaries (red lines) are flat. Blue lines show two subgrain boundaries. To enhance the image contrast, a 2D Fourier filter was applied to the projection. b) A 2.6 Å thick internal slice indicating the existence of atomic steps at the twin boundaries (red lines). The subgrain boundaries (blue lines) are two lattice spacings wider than those in (a). c) Enlarged view of a twin boundary in (b). d,e) A 2.6 Å thick slice above and below the slice of (c), revealing that the atomic steps vary in consecutive atomic layers. f) Enlarged view of a stacking fault in the 2.6 Å thick internal slice, which is in good agreement with the classical model for a face-centered-cubic extrinsic stacking fault (inset). Reprinted with permission from Ref. [24].

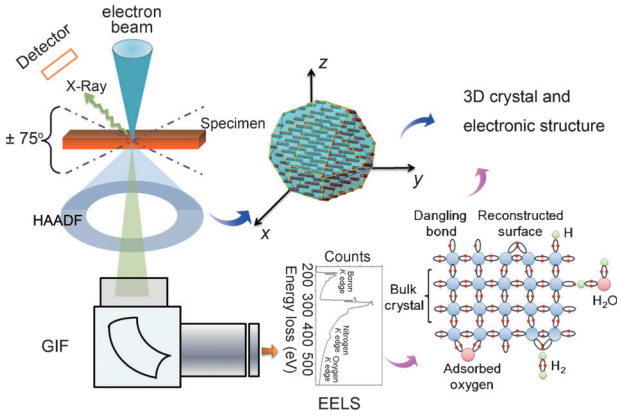

Figure 3. Illustration of ET combined with EELS in the scanning transmission electron microscope, which can be used to probe the 3D crystal and electronic structure of a nano-object. GIF = Gatan Imaging Filter.

Received: May 3, 2013
Published online: July 15, 2013

[1] J. C. Yang, M. W. Small, R. V. Grieshaber, R. G. Nuzzo, *Chem. Soc. Rev.* **2012**, *41*, 8179 – 8194.
[2] C. Li, S. Zhang, B. Zhang, D. Su, S. He, Y. Zhao, J. Liu, F. Wang, M. Wei, D. G. Evans, X. Duan, *J. Mater. Chem. A* **2013**, *1*, 2461 – 2467.
[3] L. D. Shao, B. S. Zhang, W. Zhang, D. Teschner, F. Girgsdies, R. Schlogl, D. S. Su, *Chem. Eur. J.* **2012**, *18*, 14962 – 14966.
[4] L. Shao, B. Zhang, W. Zhang, S. Y. Hong, R. Schlögl, D. S. Su, *Angew. Chem.* **2013**, *125*, 2168 – 2171; *Angew. Chem. Int. Ed.* **2013**, *52*, 2114 – 2117.
[5] B. S. Zhang, X. J. Ni, W. Zhang, L. D. Shao, Q. Zhang, F. Girgsdies, C. H. Liang, R. Schlogl, D. S. Su, *Chem. Commun.* **2011**, *47*, 10716 – 10718.
[6] W. Zhang, Q. Zhang, M.-Q. Zhao, L. T. Kuhn, *Nanotechnology* **2013**, *24*, 275301.
[7] B. Zhang, W. Zhang, L. Shao, D. S. Su, *ChemCatChem* **2013**, *5*, DOI: 10.1002/cctc.201200654.
[8] B. Zhang, L. Shao, W. Zhang, D. S. Su, *ChemCatChem* **2013**, *5*, DOI: 10.1002/cctc.201300249.
[9] B. Zhang, W. Zhang, D. S. Su, *ChemCatChem* **2011**, *3*, 965 – 968.
[10] B. S. Zhang, D. Wang, W. Zhang, D. S. Su, R. Schlogl, *Chem. Eur. J.* **2011**, *17*, 12877 – 12881.
[11] X. L. Mou, B. S. Zhang, Y. Li, L. D. Yao, X. J. Wei, D. S. Su, W. J. Shen, *Angew. Chem.* **2012**, *124*, 3044 – 3048; *Angew. Chem. Int. Ed.* **2012**, *51*, 2989 – 2993.
[12] R. Leary, P. A. Midgley, J. M. Thomas, *Acc. Chem. Res.* **2012**, *45*, 1782 – 1791.
[13] H. Friedrich, P. E. de Jongh, A. J. Verkleij, K. P. de Jong, *Chem. Rev.* **2009**, *109*, 1613 – 1629.
[14] Z. Saghi, P. A. Midgley in *Annu. Rev. Mater. Res.*, *Vol. 42* (Ed.: D. R. Clarke), Annual Reviews, Palo Alto, **2012**, pp. 59 – 79.
[15] J. M. Thomas, R. Leary, P. A. Midgley, D. J. Holland, *J. Colloid Interface Sci.* **2013**, *392*, 7 – 14.
[16] P. A. Midgley, R. E. Dunin-Borkowski, *Nat. Mater.* **2009**, *8*, 271 – 280.
[17] D. J. De Rosier, A. Klug, *Nature* **1968**, *217*, 130 – 134.
[18] V. Lučić, F. Förster, W. Baumeister, *Annu. Rev. Biochem.* **2005**, *74*, 833 – 865.
[19] R. Erni, M. D. Rossell, C. Kisielowski, U. Dahmen, *Phys. Rev. Lett.* **2009**, *102*, 09619.
[20] M. C. Scott, C. C. Chen, M. Mecklenburg, C. Zhu, R. Xu, P. Ercius, U. Dahmen, B. C. Regan, J. W. Miao, *Nature* **2012**, *483*, 444 – U491.
[21] S. Van Aert, K. J. Batenburg, M. D. Rossell, R. Erni, G. Van Tendeloo, *Nature* **2011**, *470*, 374 – 377.
[22] S. Bals, M. Casavola, M. A. van Huis, S. Van Aert, K. J. Batenburg, G. Van Tendeloo, D. Vanmaekelbergh, *Nano Lett.* **2011**, *11*, 3420 – 3424.
[23] B. Goris, S. Bals, W. Van den Broek, E. Carbo-Argibay, S. Gomez-Grana, L. M. Liz-Marzan, G. Van Tendeloo, *Nat. Mater.* **2012**, *11*, 930 – 935.
[24] C.-C. Chen, C. Zhu, E. R. White, C.-Y. Chiu, M. C. Scott, B. C. Regan, L. D. Marks, Y. Huang, J. Miao, *Nature* **2013**, *496*, 74 – 77.
[25] M. Behrens, F. Studt, I. Kasatkin, S. Kühl, M. Hävecker, F. Abild-Pedersen, S. Zander, F. Girgsdies, P. Kurr, B.-L. Kniep, M. Tovar, R. W. Fischer, J. K. Nørskov, R. Schlögl, *Science* **2012**, *336*, 893 – 897.
[26] W. Zhang, A. Trunschke, R. Schlogl, D. S. Su, *Angew. Chem.* **2010**, *122*, 6220 – 6225; *Angew. Chem. Int. Ed.* **2010**, *49*, 6084 – 6089.
[27] D. S. Su, T. Jacob, T. W. Hansen, D. Wang, R. Schlogl, B. Freitag, S. Kujawa, *Angew. Chem.* **2008**, *120*, 5083 – 5086; *Angew. Chem. Int. Ed.* **2008**, *47*, 5005 – 5008.